Impact of relative humidity variations on Carrara marble mechanical properties investigated by nonlinear resonant ultrasound spectroscopy

Marie-Laure Chavazas, Philippe Bromblet, Jérémie Berthonneau, Jérémy Hénin, Cédric Payan

Impact of relative humidity variations on Carrara marble mechanical properties investigated by Nonlinear Resonant Ultrasound Spectroscopy

Marie-Laure Chavazas[1, 2] *, Philippe Bromblet[2], Jérémie Berthonneau[2], Jérémy Hénin[3], Cédric Payan[1]

[1] Aix Marseille Univ, CNRS, Centrale Marseille, LMA UMR 7031, Marseille, France
4, impasse Nikola Tesla CS 40006 13 453 Marseille cedex 13 France

[2] Centre Interdisciplinaire de Conservation et de Restauration du Patrimoine, Marseille, France
21, rue Guibal 13 003 Marseille France

[3] Ministère de la Culture, Laboratoire de Recherche des Monuments Historiques
29, rue de Paris 77 420 Champs-sur-Marne France

* Corresponding author:
e-mail: chavazas@lma.cnrs-mrs.fr
full postal address: Marie-Laure Chavazas CICRP 21, rue Guibal 13 003 Marseille France

E-mail addresses:
- Philippe Bromblet: philippe.bromblet@cicrp.fr
- Jérémie Berthonneau: jeremie.berthonneau@cicrp.fr
- Jérémy Hénin: jeremy.henin@culture.gouv.fr
- Cédric Payan: cedric.payan@univ-amu.fr

Abstract

Like many other stones, marble mechanical properties can be significantly changed in presence of water. Water most often induces a weakening which can lead to marble degradation when coupled to temperature variations. Yet, marble artefacts are more frequently subjected to relative humidity (RH) variations than episodes of water imbibition and/or drastic temperature variations. Thus, one could wonder how do variations of RH alone impact marble mechanical state. In this study, Carrara Gioia marble samples are subjected to adsorption-desorption cycles. They were previously thermally-damaged between 40 and 105 °C, and their microstructure was characterized for each heating temperature. The evolution of their mechanical properties is monitored non-destructively with two parameters measured by Nonlinear Resonant Ultrasound Spectroscopy. The resonant frequency decreases weakly with increasing RH, indicating a diminution in sample stiffness due to low moisture-induced softening. The nonlinear parameter increases strongly, probably due to higher capillary pressure associated to a capillary condensation increase with RH. However, these phenomena are reversible: during adsorption-desorption cycling both parameters remain quite constant for a given RH. Therefore, while a RH increase impacts the mechanical properties of Carrara marble, adsorption-desorption cycling shows a reversible behavior which does not induce any permanent change in mechanical properties.

Keywords: Carrara marble, nonlinear resonant ultrasound, relative humidity, adsorption-desorption cycles

1. Introduction

Outdoor exposure can result in various deterioration patterns on built and statuary heritage made of stone [1]. More specifically, weather condition variations can be damaging for this type of material. For instance, stone artefacts exposed outdoors are subjected to frequent changes in temperature and relative humidity (RH) (day-night and seasonal variations). These cyclical fluctuations can lead to considerable damage. As an example, marble slabs can be affected by a bowing phenomenon when exposed to temperatures variations and moisture [1–4].

The presence of water alone can also significantly impact stone artefacts. Indeed, stone are porous materials that can be greatly affected by water molecules (in liquid or gaseous state) migrating within the pore spaces. As a consequence, the mechanical properties of various stone types, such as sandstones [5–8], limestones [9–14], igneous rocks [15], shales [16], are significantly changed in presence of water. Various mechanisms can be at stake depending on stone type: fracture energy reduction, capillary tension decrease, pore pressure increase, frictional reduction, chemical and corrosive deterioration [16,17]. Marble is also mechanically affected by the presence of water molecules. Mahmutoğlu (2006) shows that peak strength of Muğla marble diminishes between dry and saturated samples subjected to the same strain rate [18]. Vásárhelyi *et al.* (1999) find that Young's modulus decreases by 4%, compressive strength by 7% and tensile strength by 1% between air-dry and saturated samples of Sivac marble [19]. In Zhu *et al.* (2020), Chinese white marble exhibits a 29% reduction in average uniaxial compressive strength and a 23% reduction in average Young's modulus between dry and water-saturated samples [20]. Therefore, the influence of water saturation on the mechanical properties of different marble types have been extensively investigated. However, stone artefacts are not only subjected to water imbibition but also often to RH variations. Therefore, the impact of exposure to different RH levels and to cyclical RH fluctuations on marble mechanical properties is also important to study.

Destructive mechanical tests have their limitations to monitor mechanical properties of marble samples during adsorption-desorption cycling as they do not allow following the same sample all along the cycling process. Ultrasonic pulse velocity can overcome this restraint as it is a non-destructive technique [21]. However, this tool is ill-adapted for probing the influence of RH variations on marble samples. Indeed, Siegesmund *et al.* (2021) show on Blanco Macael marble that changes in RH levels do not significantly affect ultrasonic pulse velocity [22]. On the contrary, Nonlinear Resonant Ultrasound Spectroscopy (NRUS) is sensitive to any change occurring at the microstructural scale, including ones due to RH fluctuations. It is a resonance method which allows monitoring the mechanical state of materials non-destructively. It is well-suited to stones in which nonlinear phenomena occur when the excitation amplitude increases, since stones are part of the nonclassical nonlinear class of materials which is characterized by hysteresis, slow dynamics, end-point memory [23–27]. So far, the influence of water saturation and RH on the nonlinear responses has been investigated in a few studies on glass bead, sand, limestone and sandstone [23,26,28–31] but not on marble. Besides, to the authors' knowledge, the impact of RH changes on the NRUS response of rocks with different damage degrees has not been yet investigated.

This work thus aims at evaluating the impact of exposure to cyclical RH fluctuations on Carrara marble, as well as the effect of the coupling between thermal damage and exposure to RH fluctuations. First, microstructural characterizations (mercury intrusion porosimetry, SEM) were conducted on the studied fresh and thermally-damaged marble samples. The influence of RH changes on the decay of Carrara Gioia marble was then monitored using NRUS. Resonant frequency and nonclassical nonlinear parameter were measured at different RH levels during adsorption and desorption on marble samples with different thermal weathering degrees. They were then also measured as samples underwent adsorption-desorption cycles between 12% and 96% RH to simulate cyclical variations. The evolution of the NRUS parameters are eventually discussed in light of marble sample microstructures.

2. Materials and methods

2.1. Sample preparation

Five core samples of Carrara Gioia marble of 20 cm in height and 4 cm in diameter were studied. They were drilled from a fresh block of Carrara Gioia marble (provided by Logica SRL, Carrara, Italy), which is a calcitic white veined marble and has a granoblastic equigranular-polygonal microstructure. The sample faces were polished to ensure flat and parallel surfaces for measurement. Four of the samples underwent a thermal treatment at respectively 40, 65, 85 and 105 °C, and one sample remained unheated. The heating rate of the oven was set to 1 °C·min^{-1} to allow the homogeneous heating of the material [22,32,33], the setpoint temperature was maintained for 6 h [22] and the cooling down to room temperature was left free. All five samples were then stored at 23 °C in temperature-controlled oven.

2.2. Microstructural characterization

Microstructural analyses were carried out on core samples drilled from the same marble block and having undergone the same thermal treatments. Marble porous network was characterized with mercury intrusion porosimetry using an AutoPore IV 9500 (Micromeritics) working with a maximal pressure of 210 MPa, thus probing pores between 0.01 and 360 µm. Mercury intrusion was measured at 111 increasing pressure points. Freshly cut fragments of thermally-damaged marble samples were also characterized under a Scanning Electron Microscope (SEM, ZEISS EVO 15).

Vapor sorption behavior was characterized along adsorption for all the samples using the 8 supersaturated salt solutions listed in section 2.3. Measurements were carried out on cylindrical slices of 4 cm in diameter and of about 1 cm in thickness. The experiment was done at 23 °C, in a temperature-controlled oven. One slice was used per sample. The dry masses were measured after the slices were under 3% RH (controlled by silica gel). The experimental points were fitted with the GAB theoretical modeling.

2.3. Experimental set-up

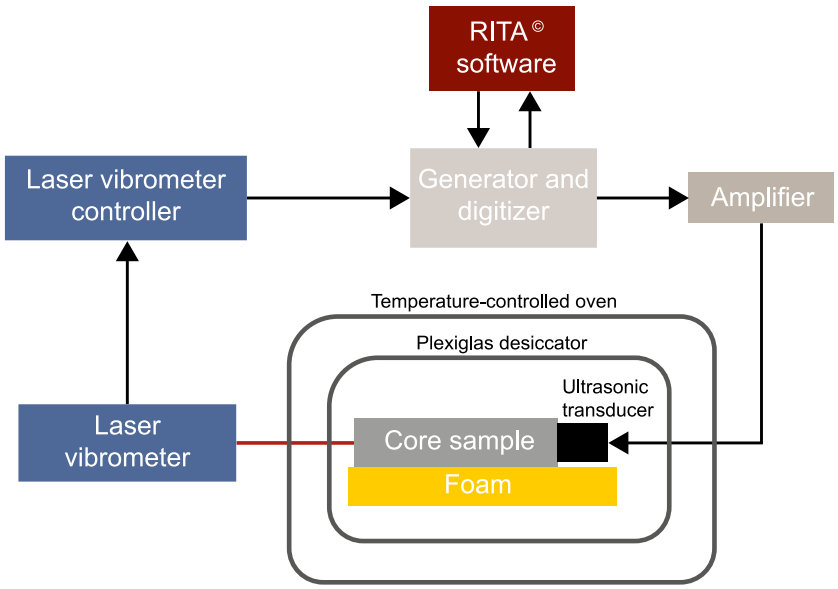

Fig. 1 (Color online) Scheme of the experimental set-up.

Fig. 2 (Color online) Sample disposition in the experimental set-up. This picture corresponds to the temperature-controlled oven and laser vibrometer part of the scheme of Fig. 1.

Fig. 1 illustrates the experimental set-up for the NRUS experiments, and Fig. 2 specifically shows sample disposition in the experimental set-up. The signal generation is managed by RITA© software coupled with a generator (NI PXIe-5406) and an amplifier (NF Electronic Instruments 4005 High Speed). The vibrations are generated in the core sample thanks to a piezoelectric transducer (Beijing Ultrasonic, resonant frequency of 40 kHz) which is permanently glued to one sample extremity with epoxy Araldite® 2020. The piezoelectric devices and the unsheathed wires are wrapped in stretch film to avoid deterioration due to high humidity levels. Samples are placed on the two middle racks of a four-level desiccator cabinet (no. 1 in Fig. 2). They are put on foam to minimize the attenuation or modification of the vibration modes due to the rigid support. On the lowest and highest racks of the desiccator, two containers with supersaturated salt solutions (no. 2 in Fig. 2) are placed to control RH inside the desiccator. The following salts are used throughout the experiments (equilibrium humidity is bracketed): LiCl (12%), $MgCl_2$ (33%), K_2CO_3 (44%), $Mg(NO_3)_2$ (52%), $NaNO_2$ (66%), NaCl (76%), KCl (86%) and K_2SO_4 (96%). The desiccator cabinet is itself placed in a temperature-controlled oven maintained at 23 °C (no. 3 in Fig. 2). This configuration was maintained during the NRUS testing: the samples were not taken out of the desiccator cabinet nor of the oven for the NRUS tests. Indeed, the out-of-plane velocity is measured at the sample extremity opposite to the piezoelectric transducer with a Polytec laser vibrometer (no. 4 in Fig. 2) (OFV-505 Single Point Sensor Head and OFV-5000 Controller, λ = 633 nm (He-Ne), power < 1 mW), which allows carrying out measurements through the interior glass door of the temperature-controlled oven and through the Plexiglas wall of the desiccator. The exterior steel doors of the temperature-controlled oven are left open during measurements to allow the laser going through. The signal acquisition is managed by RITA© software coupled with a digitizer (NI PXIe-5122). The NRUS measurements were made after the samples had been exposed under a specific RH for at least 48 h to ensure stabilization of equilibrium humidity inside the desiccator (controlled by an iButton® temperature-humidity logger). At least three NRUS tests were performed on each sample at each ambient RH, waiting at least 3 h between two scans on the same sample in order to avoid slow dynamic processes influence [24,26,27,34].

2.4. Nonlinear Resonant Ultrasound Spectroscopy (NRUS)

NRUS is a resonance technique in which a sample is excited at different increasing amplitudes to study the evolution of its resonant modes. Marble belongs to the nonclassical nonlinear class of materials, which means that its modulus *K* is in the form [25–28]:

$$K = K_0[1 + \beta\varepsilon + \delta\varepsilon^2 + \cdots + \alpha(\Delta\varepsilon, \dot{\varepsilon})] \quad (1)$$

where K_0 is the elastic modulus, β and δ are the classical nonlinear coefficients and α is the nonclassical nonlinear parameter. As marble is a nonlinear material, its resonant frequency for a given mode is shifted towards low frequencies as the drive amplitude increases. This phenomenon can be observed on the NRUS scan for the unheated Carrara Gioia marble sample under 12% RH displayed on Fig. 3. Relative shift frequency is proportional to the strain amplitude $\Delta\varepsilon$ of the sample, with the nonclassical nonlinear parameter α as the proportionality coefficient [35,36]:

$$\Delta f / f_0 = \alpha \, \Delta\varepsilon \qquad (2)$$

where $\Delta f = f_0 - f$ with f_0 the linear resonant frequency (obtained for the lowest drive amplitude) and f the resonant frequency for higher drive amplitudes. In this study, only the first longitudinal mode of marble samples is investigated. The strain $\Delta\varepsilon$ reached at resonance peaks is evaluated from the out-of-plane particle velocity amplitude A recorded by the vibrometer at resonance:

$$\Delta\varepsilon = A/(2 * L * f_0) \qquad (3)$$

where L is the sample length and f_0 is the low amplitude resonant frequency.

Therefore, NRUS provides two useful parameters to characterize any nonclassical nonlinear material such as marble:

- The resonant frequency f_0 (linear resonant frequency extracted for the lowest drive amplitude) which is related to the stiffness and density of the macroscopic sample,
- The nonlinear parameter α which is highly sensitive to any change at the microstructural scale, such as microcracks, capillary effects, friction, contacts, dislocations [23,37–39].

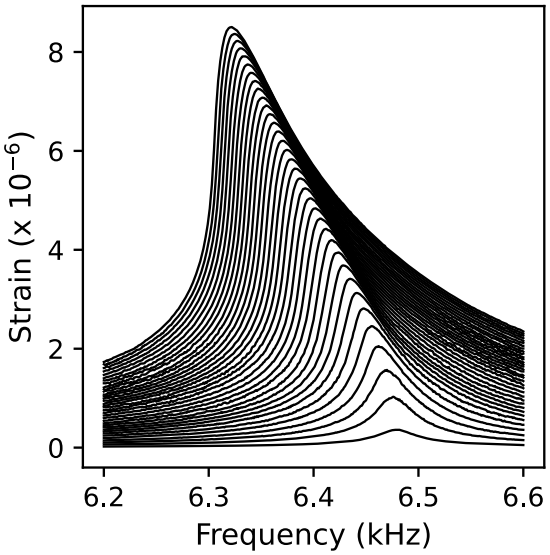

Fig. 3 NRUS curves obtained for the unheated Carrara Gioia marble sample under 12% RH. Resonant frequency f_0 is of 6479.9 ± 0.7 Hz and nonlinear parameter α of (3.5 ± 0.5) × 10^3. One single curve corresponds to one drive amplitude level. The resonant frequency shift towards low frequencies is noticeable, as well as its proportionality with the strain reached at resonance for the highest drive amplitudes.

3. Results

3.1. Microstructural impact of thermal treatment

The evolutions of total porosity and pore size distribution with setpoint temperature of thermal treatment are respectively displayed on Fig. 4 and Fig. 5, and are summarized in Table 1. One can note the global increase in porosity with heating temperature, from 0.81% for the unheated sample to 2.59% for the sample heated at 105 °C (Fig. 4). Fig. 5 shows an increase in the radius of pore access with heating temperature. Indeed, the contribution of pores with access radius between 0.01 and 1 µm diminishes for the benefit of wider pores (> 1 µm) as heating temperature increases.

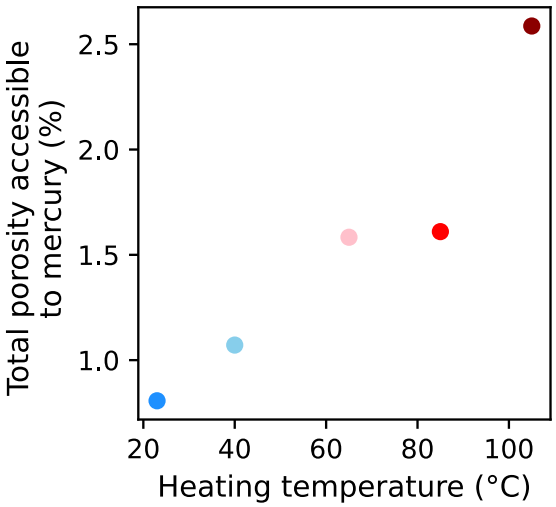

Fig. 4 (Color online) Total porosity (accessible to mercury) of Carrara marble samples heated at different temperatures.

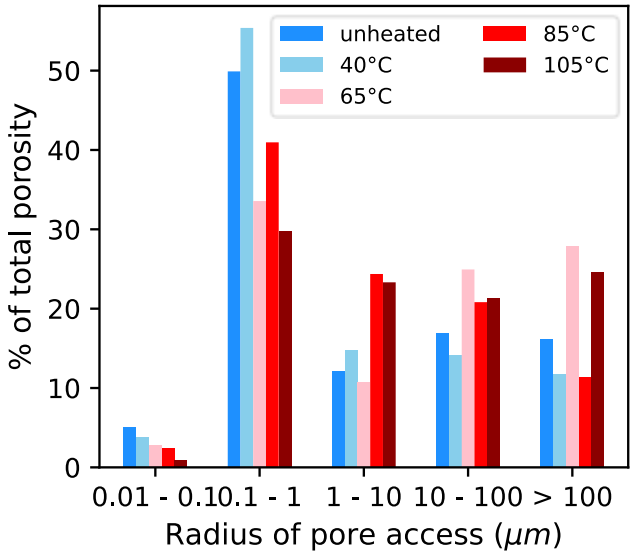

Fig. 5 (Color online) Porosity classes for Carrara marble samples heated at different temperatures. Contribution of five porosity classes (radius of pore access between 0.01 and 0.1 µm, between 0.1 and 1 µm, between 1 and 10 µm, between 10 and100 µm, and above 100 µm) to the global porosity of Carrara marble samples.

Fig. 6 shows SEM images of pores for the unheated sample and the sample heated at 85 °C. It highlights the presence of intergranular spaces even in unheated Carrara marble samples, and their widening due to heating.

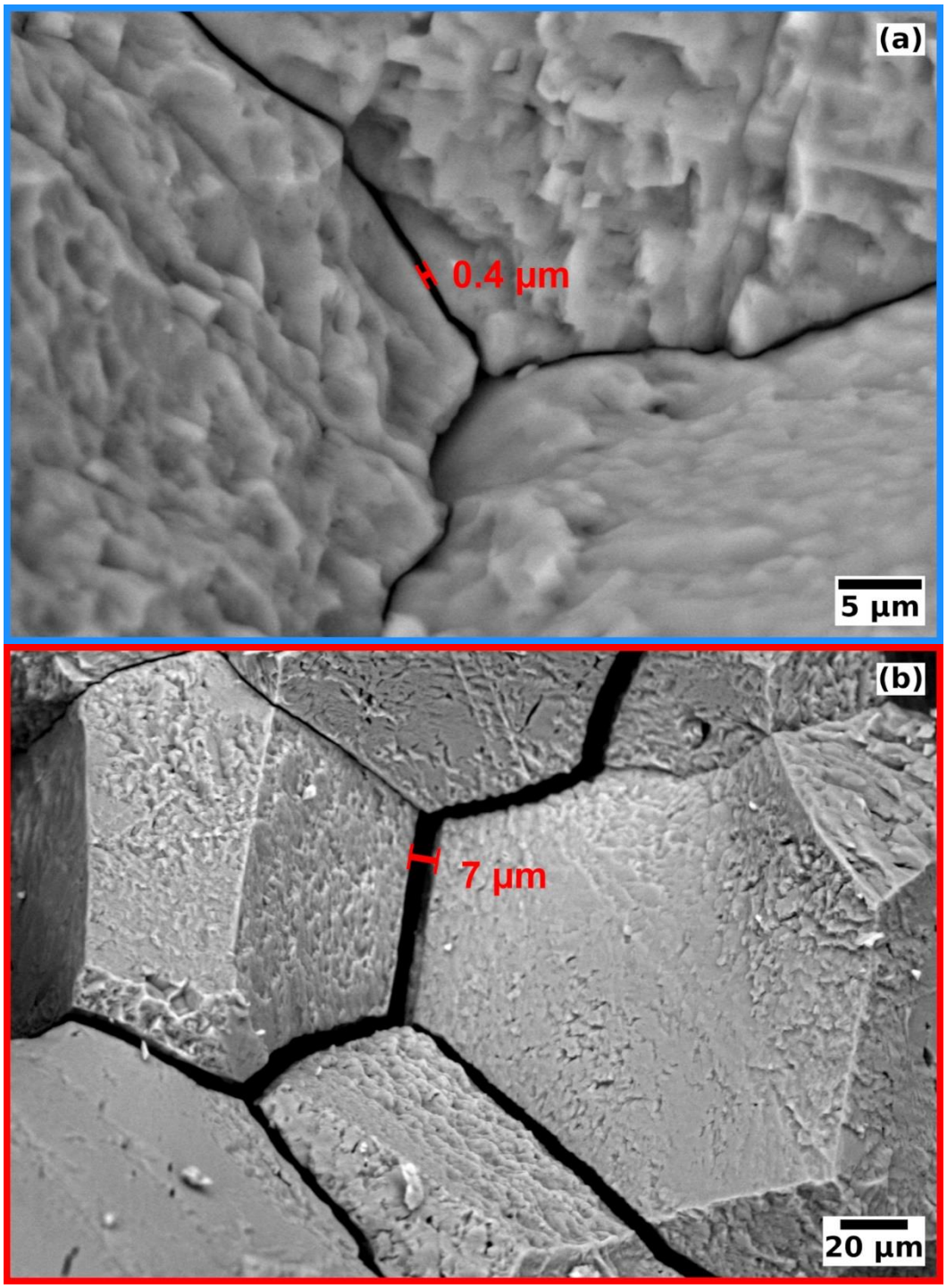

Fig. 6 (Color online) SEM images (magnification (a) x2000, (b) x400) on fracture plans of Carrara Gioia marble for (a) unheated sample and (b) sample heated at 85 °C. Indications of the width of the intergranular spaces is given in red.

Sorption isotherms are displayed on Fig. 7. The water uptake is the lowest for the sample heated at 105 °C and the highest for the unheated sample and the sample heated at 40 °C with the samples heated at 65 and 85 °C in between. The increase in water content with RH at a given heating temperature can be explained by the capillary condensation occurring at highest RH. One can note that, for a given value of RH, water content tends to decrease with heating temperature. It can be linked to the widening of pores access radius (Fig. 5, Fig. 6) when heating temperature increases, as less small pores are available for capillary condensation to occur.

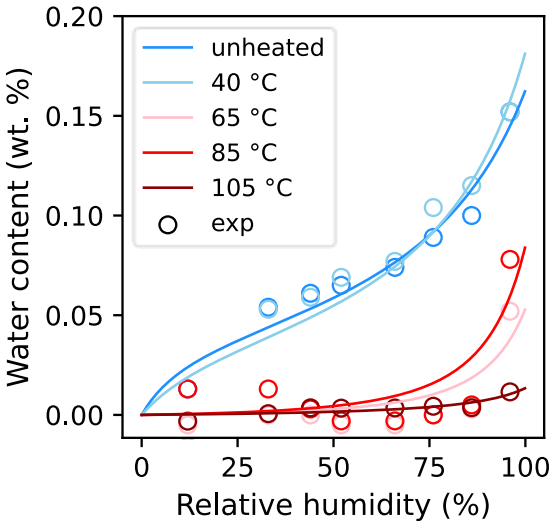

Fig. 7 (Color online) Sorption isotherms for the Carrara marble samples heated at different temperatures.

3.2. Impact of relative humidity: adsorption

The five Carrara marble samples were exposed to the relative humidities listed in section 2.3 in increasing order (from 12% to 96%). Fig. 8 (a) and (b) present for each sample the evolution of its resonant frequency f_0 and of its nonlinear parameter α with RH. A data point corresponds to the average value of the studied parameter for all NRUS scans performed at a given RH on the sample. The uncertainties (shaded areas in Fig. 8) correspond to one standard deviation. The data spread is very low for the resonant frequency f_0 and higher for the nonlinear parameter α. Relative changes in resonant frequency f_0 and nonlinear parameter α for each sample are shown in Fig. 9, the reference value being the parameter value at 12% RH. In Fig. 10, the relative changes are also given as a function of the relative changes in sample water content (reference value is the value at 12% RH for both axes).

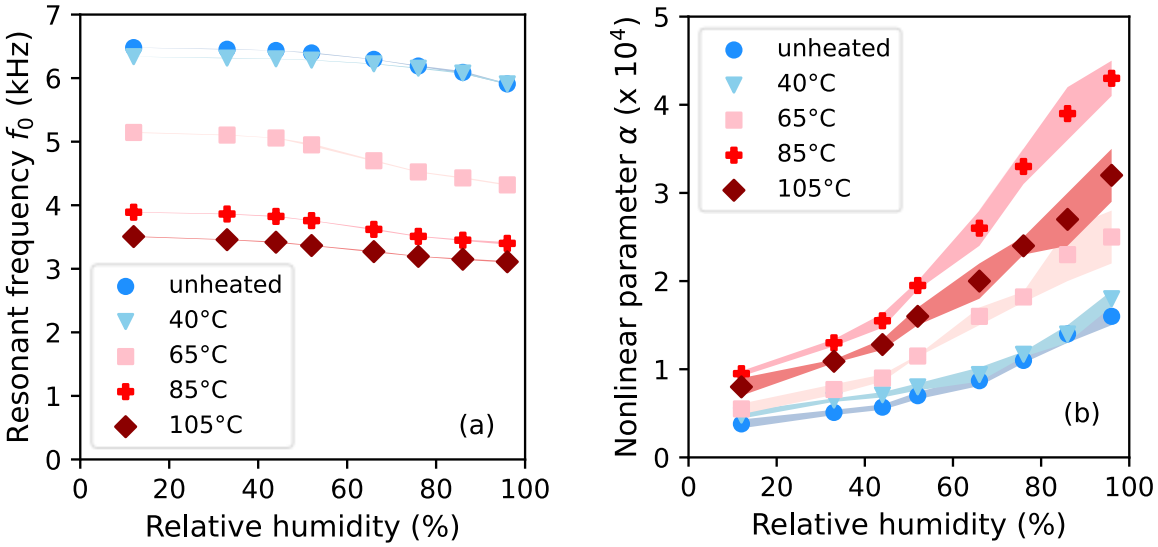

Fig. 8 (Color online) Evolution of the NRUS parameters during adsorption. (a) Resonant frequency f_0 and (b) nonlinear parameter α as a function of RH for Carrara Gioia marble samples previously heated at various temperatures. Shaded areas denote one standard deviation.

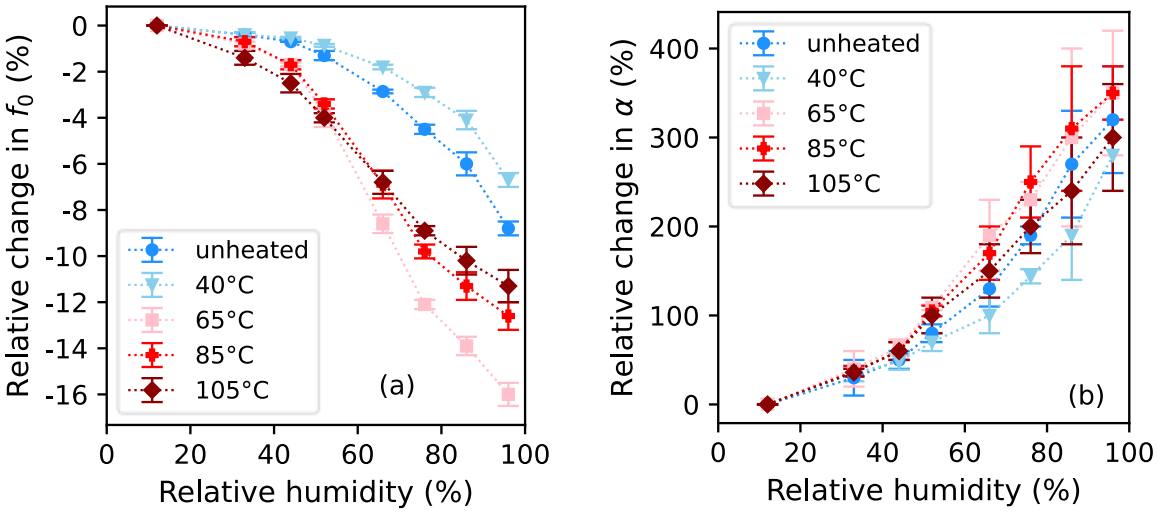

Fig. 9 (Color online) Variation of the NRUS parameters during adsorption. Relative change in (a) resonant frequency f_0 and (b) nonlinear parameter α with RH during adsorption for Carrara marble samples previously heated at various temperatures.

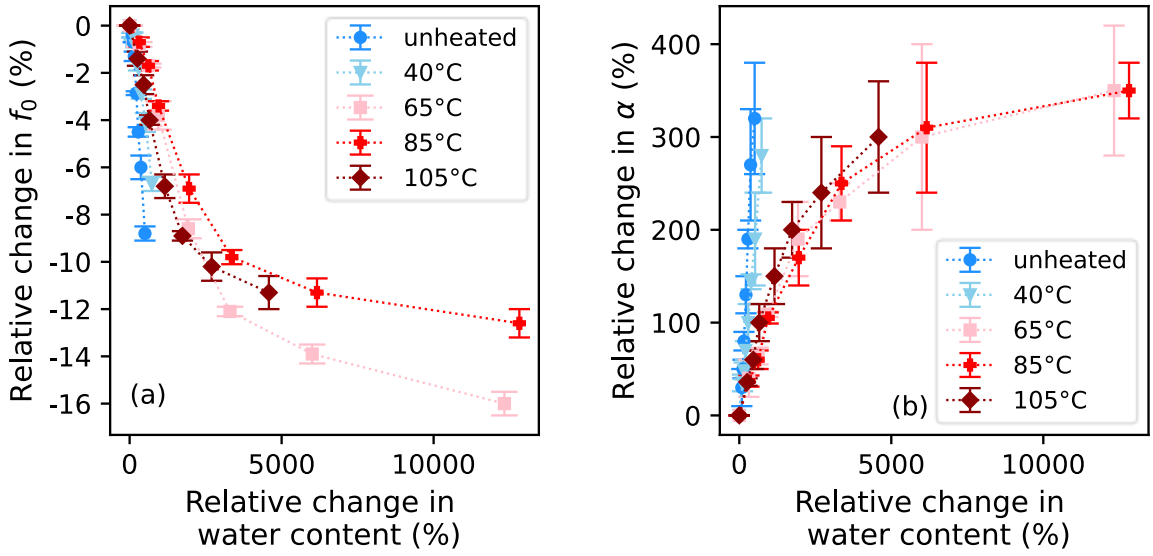

Fig. 10 (Color online) Variation of the NRUS parameters during adsorption. Relative change in (a) resonant frequency f_0 and (b) nonlinear parameter α as a function of the relative change in water content during adsorption for Carrara marble samples previously heated at various temperatures.

For all the samples, the resonant frequency f_0 tends to slightly decrease as RH increases (Fig. ***8***). For a given air humidity, the resonant frequency f_0 is always the highest for the unheated and the 40 °C heated samples, then it gradually diminishes for samples heated at 65, 85 and 105°C. For the unheated sample, the resonant frequency f_0 reduces from 6.4801 ± 0.0007 kHz at 12% RH to 5.909 ± 0.008 kHz at 96% RH. For the sample heated at 105°C, it decreases from 3.507 ± 0.006 kHz at 12% RH to 3.11 ± 0.01 kHz at 96% RH. Between 12% and 96% RH, the resonant frequency f_0 globally decreases by 9%, 7%, 16%, 13% and 11%, respectively for the unheated sample and the samples heated at 40, 65, 85 and 105°C (Fig. 9). For a given increase in water content, samples exhibit comparable relative changes in resonant frequency f_0 (Fig. 10).

The nonlinear parameter α increases with increasing RH for all the samples (Fig. 8). For a specific RH, the highest value of nonlinear parameter α is always reached for the sample heated at 85°C and the lowest is reached for the unheated sample. Between them two, the value of the nonlinear parameter α increases in this order: samples heated at 40, 65 and 105°C. For the unheated sample, at 12% RH the nonlinear parameter α is evaluated at $(3.8 \pm 0.5) \times 10^3$ and reaches $(16 \pm 1) \times 10^3$ at 96% RH. Between 12% and 96% RH, the nonlinear parameter α of the sample heated at 85°C rises from $(9.5 \pm 0.3) \times 10^3$ to $(43 \pm 2) \times 10^3$. Between 12% RH and 96%, the nonlinear parameter α globally increases by 320%, 280%, 350%, 350% and 300%, respectively for the unheated sample and the samples heated at 40, 65, 85 and 105°C (Fig. 9). Samples do not reach the same levels of increase in nonlinear parameter α at a given increase in water content: the highest is reached for the unheated sample and the sample heated at 40 °C, followed by the samples heated at 65, 85 and 105 °C (Fig. 10).

3.3. Adsorption-desorption cycles

The evolution of the NRUS parameters was also investigated during desorption for the unheated and 85 °C heated samples to study a complete adsorption-desorption cycle. The samples were exposed to the relative humidities listed in section 2.3 in decreasing order (from 96% to 12%). The results are presented in Fig. 11. Fig. 11 (a) and (b) display the evolution of the resonant frequency f_0 and of the nonlinear parameter α with RH during adsorption (empty black circles) and desorption (filled blue circles) for the unheated sample. The same evolutions are presented for the sample heated at 85 °C in Fig. 11 (c) and (d) (empty black crosses for adsorption, filled red crosses for desorption). For a given RH level, the resonant frequency values are extremely similar during adsorption and desorption phases for the two samples. They only differ at 12% and 33% RH for the sample heated at 85 °C. In contrast, the nonlinear parameter values do not coincide during the two phases for intermediate relative humidities for none of the samples.

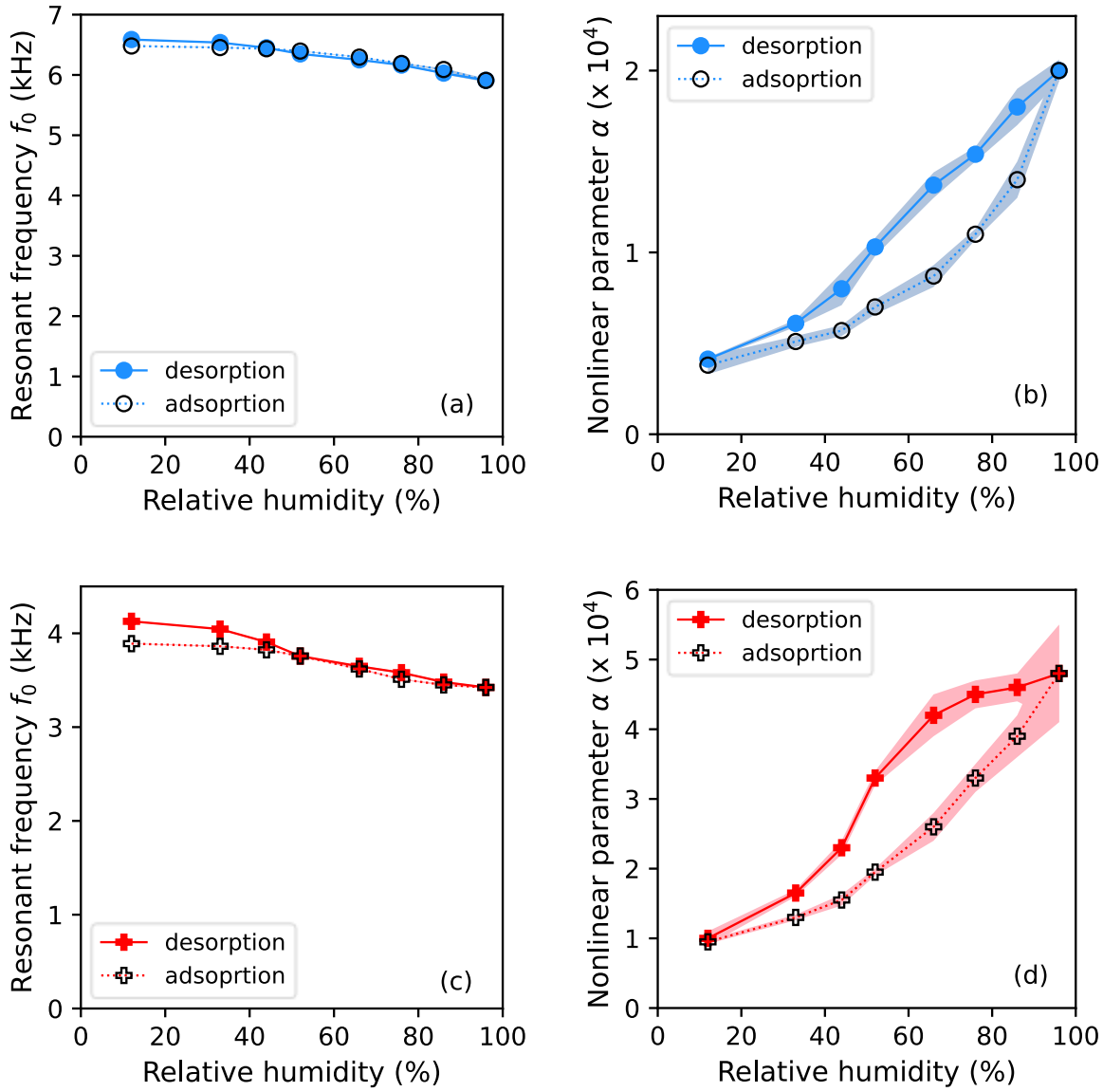

Fig. 11 (Color online) Adsorption-desorption cycle. Evolution of the resonant frequency f_0 (on the left) and of the nonlinear parameter α (on the right) with RH during adsorption (empty symbols) and desorption (filled symbols) for the (a, b) unheated (blue circles) and (c, d) 85 °C heated (red crosses) samples. Shaded areas denote one standard deviation.

The evolution of the NRUS parameters at 12% and 96% RH was also followed during 10 adsorption-desorption cycles for the five samples to verify whether the effects of RH changes on the resonant frequency f_0 and the nonlinear parameter α could be reversible. The results are displayed on Fig. 12. Fig. 12 (a) and (b) present the evolution of the resonant frequency f_0 and of the nonlinear parameter α at 12% RH during 10 adsorption-desorption cycles. Fig. 12 (c) and (d) present the same evolutions at 96% RH. Dashed lines correspond to average values of the NRUS parameters over the 10 cycles. Data for the second cycle lack for samples heated at 40, 65 and 105 °C because they were not measured. The resonant frequency f_0 slightly increases at 12% RH over the 10 cycles and remains steady at 96% RH. At 12% and 96% RH, the nonlinear parameter α varies around the average but without exhibiting an overall tendency to increase or decrease during cycling.

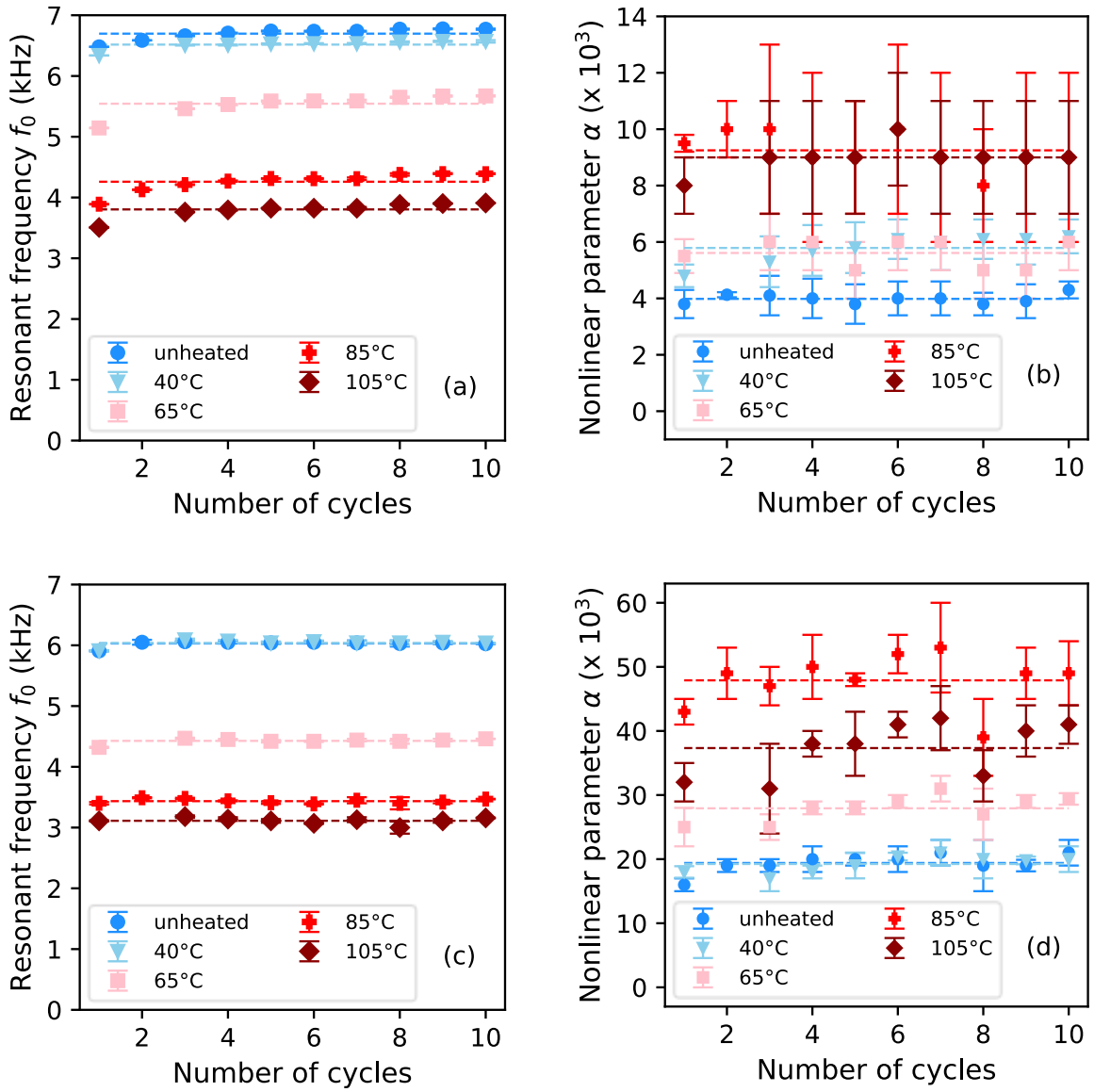

Fig. 12 (Color online) Adsorption-desorption cycling. Evolution of the resonant frequency f_0 (on the left) and of the nonlinear parameter α (on the right) at (a, b) 12% RH and (c, d) 96% RH during 10 adsorption-desorption cycles for marble samples previously heated at various temperatures. Dashed lines correspond to average values of the parameter over the 10 cycles and are given for information.

4. Discussion

Marble artefacts undergo various deterioration patterns when exposed to cyclical thermo-hygric variations. Yet, the sole impact of RH fluctuations remained unknown. Its influence has thus been investigated with NRUS and the results show the role of moisture-induced softening and capillary condensation. They also show that RH cycling does not lead to permanent deterioration in Carrara marble regardless of its damage state.

One can first note the difference in the sensitivity of the resonant frequency f_0 and the nonlinear parameter α to RH changes (Fig. 8, Fig. 9). This observation is consistent with previous studies on granular materials. In Siegesmund *et al.* (2021), the influence of air humidity on ultrasonic velocity in marble is found to be low [22]. Compressional wave velocity V_P is closely linked to the resonant

frequency f_0 of the longitudinal mode: $V_P = 2 * L * f_0$, L being the sample length. Moreover, Ostrovsky and Johnson (2001) emphasize that the nonlinear parameter α is more dependent on water presence than linear parameters in geomaterials [23]. It is also in agreement with findings on a medium made of glass beads in which linear wave velocity is not affected by RH changes while all the nonlinear parameters (α, β, γ) increase with increasing RH [31].

The resonant frequency f_0 of Carrara marble samples decreases by between 7 and 16% as RH increases between 12% and 96% whatever the heating temperature (Fig. 9 (a)). This decrease of the resonant frequency f_0 could be explained by the moisture-induced softening of stones: the reduction of their mechanical strength in presence of water [40]. Studies have shown that mechanical properties (Young's modulus, compressive and tensile strength) of marble are reduced when the samples are water saturated [18–20]. While generally considered as a result of liquid water, this work shows that this reduction occurs even along RH changes corresponding to very low water content (between 0.01 and 0.18 wt. %). This diminution of the resonant frequency f_0 at low water content could correspond to the onset of moisture-induced softening in Carrara marble: water inside pores can weaken friction between grains, thus inducing sliding between them and reducing mechanical properties.

Regarding the nonlinear parameter α, it can first be noticed that this parameter is affected by a hysteresis phenomenon during adsorption-desorption cycles. Indeed, values reached during the desorption phase do not correspond to the ones of the adsorption phase (Fig. 11). Hysteresis loops during an adsorption-desorption cycle are well-known in sorption isotherms and are due to different mechanisms occurring during adsorption and desorption, such as a reduction of contact angle from adsorption to desorption, delay in meniscus formation, condensate trapped in ink bottle pores [41]. These different mechanisms occurring at the microscopic scale could also affect the nonlinear parameter α and lead to the presence of a hysteresis loop between adsorption and desorption phases. Therefore, values of the nonlinear parameter α measured at a given RH depend on the sample history regarding moisture uptake or release.

Besides, the nonlinear parameter α exhibits a significant increase with increasing RH: by between 280% and 350% from 12% to 96% RH. This increase corroborates observations made on other granular materials. In Johnson *et al.* (2004), the nonlinear parameter α increases with water saturation in St. Pantaleon limestone. In Meule sandstone, it increases for saturations below 30% and then slowly decreases [26]. Averbakh *et al.* (2017) show that the nonlinear parameter α of longitudinal mode increases with increasing water saturation for an unspecified limestone [29]. Van Den Abeele *et al.* (2002) find that the nonlinear parameter α first increases with increasing water saturation in Lavoux limestone and Berea and Meule sandstones, and then levels off at highest saturations [28]. Gao *et al.* (2023) find that the nonlinear parameter α increases with RH in glass beads but not in sand where it remains constant [30]. Authors hypothesize that this difference in behavior comes from more grain interlocking in sand which prevents adsorbed water from weakening/dilating the sample, unlike in glass beads [30]. Van Den Abeele *et al.* (2002) explain the increase in nonlinearity with increasing water saturation by the presence of capillary condensation. Capillary condensation does not appear simultaneously in the whole pore network as it depends on the pore radius via Kelvin's law. Therefore, menisci are formed at the interfaces of air and liquid water and these menisci are subjected to microscopic capillary pressure because of the difference between the pressure in air and in liquid water. Microscopic capillary pressure results in a microscopic contraction pressure in the solid matrix where the menisci are formed. These microscopic forces occurring in the pore network can lead to an additional nonlinearity when samples are subjected to an increasing RH. Microscopic forces due to capillary condensation could also explain the increase of nonlinearity with RH in this work as water molecules can penetrate the intergranular spaces which are present in all the studied samples (Fig. 6).

However, it can be noted on Fig. 9 that relative changes in nonlinear parameter α (and in resonant frequency f_o) do not seem correlated with the total amount of porosity in sample (Fig. 4), pore size distribution (Fig. 5, Fig. 6), or water content (Fig. 7). Relative changes are of the same order of magnitude for all the samples whereas one could have expected that some of the samples exhibit more relative variations of nonlinearity than others due to their different pore network (Fig. 4, Fig. 5, Fig. 6). As capillary condensation is conditioned by Kelvin's law, a study of pore proportion below and above Kelvin's radius in the studied marble samples could have been insightful. Unfortunately, for water as the fluid and at 25 °C, Kelvin's radius ranges from 4.95×10^{-4} to 2.57×10^{-2} µm for RH between 12%

and 96%, which is below the pore radius detected by mercury intrusion porosimetry on the studied samples. The sorption isotherms can still give a first insight (Fig. 7). They highlight that less capillary condensation occurs in the samples heated at 65, 85 and 105 °C than in those unheated and heated at 40 °C, even though all these samples display similar increase of nonlinearity. Therefore, for the same water content, the relative changes in the nonlinear parameter α (and in the resonant frequency f_0) are extremely dissimilar between each samples. Nonetheless, Fig. 10 shows that more comparable increases of the nonlinear parameter α and very similar decreases of the resonant frequency f_0 are reached for a given relative change in water content. Therefore, the NRUS parameters could be more affected by water content variations than by the absolute water content amount within the samples.

After one adsorption-desorption cycle, changes caused in the resonant frequency f_0 and in the nonlinear parameter α by RH fluctuations seem reversible as similar values for the nonlinear parameter α are reached at 12% RH at the beginning and at the end of the adsorption-desorption cycle (Fig. 11). The evolutions of the resonant frequency f_0 and of the nonlinear parameter α were therefore followed during 10 adsorption-desorption cycles (Fig. 12) to verify this hypothesis on a longer-term experiment. Overall, the results tend to validate the hypothesis of reversibility (Fig. 12). The resonant frequency f_0 at 12% RH displays a slight increase during cycling (up to 13% for the sample heated at 85 °C). However, it remains constant at 96% RH for all the samples. The nonlinear parameter α at 12% and 96% RH does not remain completely steady during cycling. Nevertheless, it does not exhibit any overall tendency to increase or decrease. It varies around the average value while remaining within the uncertainty range. Therefore, the nonlinear parameter α does not seem permanently affected by RH variation: same values are reached when returning to the initial RH level. Thus, fresh as well as thermally-damaged marble samples exhibit a reversible behavior with RH variations. Therefore, climatic RH fluctuations alone do not seem able to lead to a permanent weakening or deformation of Carrara Gioia marble.

5. Conclusions

The effects of RH variations on Carrara Gioia marble were investigated with NRUS through the evolution of the resonant frequency f_0 and of the nonlinear parameter α during single and multiple adsorption-desorption cycles. The impact of the coupling between thermal damage and exposure to RH fluctuations is also investigated as Carrara marble samples were previously thermally-damaged by heating between 40 and 105 °C.

The decrease of the resonant frequency f_0 with increasing RH could reflect the onset of moisture-induced softening. The nonlinear parameter α is extremely sensitive to RH changes and is affected by hysteretic phenomena occurring during adsorption-desorption cycle. The increase in nonlinearity with RH could be due to capillary condensation occurring in pore network. The intensity of NRUS parameters variation seems more linked to water content variation than to thermal damage degree (and therefore total amount of porosity) or to absolute water content.

Nonetheless, adsorption-desorption cycling does not lead to an overall significant decrease or increase of the resonant frequency f_0 or of the nonlinear parameter α. Therefore, under stable temperature conditions, microstructural phenomena at stake in Carrara Gioia samples subjected to RH variations could be reversible. This work shows that exposure to cyclical RH fluctuations alone cannot lead to permanent weakening/deformation of Carrara marble. This reversibility is observed for five increasing degrees of thermal deterioration, meaning that RH cycling does not permanently impact Carrara marble no matter its degradation state. Nevertheless, RH variations could play a role to initiate or enhance some alterations when they are coupled to other agents (salt crystallizations, thermal variations, etc.).

Author contributions

Conceptualization, P.B., J.B., C.P.; supervision, P.B., J.B., C.P.; investigation, M.L.C., J.H.; visualization, M.L.C.; writing – original draft, M.L.C.; writing – review & editing, M.L.C., P.B., J.B., C.P.

Competing interests statement

The authors declare that they have no known competing financial interests or personal relationships that could have appeared to influence the work reported in this paper.

Funding sources

This research did not receive any specific grant from funding agencies in the public, commercial, or not-for-profit sectors.

Acknowledgements

Authors wish to thank Alain Tonetto and Louis Godaert (PRATIM, Aix Marseille Univ, France) for their help with the SEM observations.

References

[1] ICOMOS-ISCS, Illustrated glossary on stone deterioration patterns - Glossaire illustré sur les formes d'altération de la pierre, Paris, 2008.

[2] B. Grelk, P. Goltermann, B. Schouenborg, A. Koch, L. Alneas, The laboratory testing of potential bowing and expansion of marble, in: Proceedings of the International Conference on Dimension Stone, Taylor & Francis Group plc, A.A. Balkerma Publische, Prague, Czech Republic, 2004: pp. 253–259.

[3] A. Koch, S. Siegesmund, The combined effect of moisture and temperature on the anomalous expansion behaviour of marble, Env Geol 46 (2004). https://doi.org/10.1007/s00254-004-1037-9.

[4] S. Siegesmund, J. Ruedrich, A. Koch, Marble bowing: comparative studies of three different public building facades, Environ Geol 56 (2008) 473–494. https://doi.org/10.1007/s00254-008-1307-z.

[5] M.L. Lin, F.S. Jeng, L.S. Tsai, T.H. Huang, Wetting weakening of tertiary sandstones—microscopic mechanism, Environ Geol 48 (2005) 265–275. https://doi.org/10.1007/s00254-005-1318-y.

[6] X. Li, K. Peng, J. Peng, D. Hou, Experimental investigation of cyclic wetting-drying effect on mechanical behavior of a medium-grained sandstone, Engineering Geology 293 (2021) 106335. https://doi.org/10.1016/j.enggeo.2021.106335.

[7] H. Li, Y. Qiao, R. Shen, M. He, T. Cheng, Y. Xiao, J. Tang, Effect of water on mechanical behavior and acoustic emission response of sandstone during loading process: phenomenon and mechanism, Engineering Geology 294 (2021) 106386. https://doi.org/10.1016/j.enggeo.2021.106386.

[8] E. Verstrynge, R. Adriaens, J. Elsen, K. Van Balen, Multi-scale analysis on the influence of moisture on the mechanical behavior of ferruginous sandstone, Construction and Building Materials 54 (2014) 78–90. https://doi.org/10.1016/j.conbuildmat.2013.12.024.

[9] J. Berthonneau, P. Bromblet, F. Cherblanc, E. Ferrage, J.-M. Vallet, O. Grauby, The spalling decay of building bioclastic limestones of Provence (South East of France): From clay minerals swelling to hydric dilation, Journal of Cultural Heritage 17 (2016) 53–60. https://doi.org/10.1016/j.culher.2015.05.004.
[10] F. Cherblanc, J. Berthonneau, P. Bromblet, V. Huon, Influence of Water Content on the Mechanical Behaviour of Limestone: Role of the Clay Minerals Content, Rock Mech Rock Eng 49 (2016) 2033–2042. https://doi.org/10.1007/s00603-015-0911-y.
[11] S. Taibi, A. Duperret, J.-M. Fleureau, The effect of suction on the hydro-mechanical behaviour of chalk rocks, Engineering Geology 106 (2009) 40–50. https://doi.org/10.1016/j.enggeo.2009.02.012.
[12] Á. Török, B. Vásárhelyi, The influence of fabric and water content on selected rock mechanical parameters of travertine, examples from Hungary, Engineering Geology 115 (2010) 237–245. https://doi.org/10.1016/j.enggeo.2010.01.005.
[13] Á. Rabat, M. Cano, R. Tomás, Effect of water saturation on strength and deformability of building calcarenite stones: Correlations with their physical properties, Construction and Building Materials 232 (2020) 117259. https://doi.org/10.1016/j.conbuildmat.2019.117259.
[14] Á. Rabat, R. Tomás, M. Cano, Evaluation of mechanical weakening of calcarenite building stones due to environmental relative humidity using the vapour equilibrium technique, Engineering Geology 278 (2020) 105849. https://doi.org/10.1016/j.enggeo.2020.105849.
[15] S. Yasar, Long term wetting characteristics and saturation induced strength reduction of some igneous rocks, Environ Earth Sci 79 (2020) 353. https://doi.org/10.1007/s12665-020-09105-0.
[16] E.M. Van Eeckhout, The mechanisms of strength reduction due to moisture in coal mine shales, International Journal of Rock Mechanics and Mining Sciences & Geomechanics Abstracts 13 (1976) 61–67. https://doi.org/10.1016/0148-9062(76)90705-1.
[17] X. Cai, Z. Zhou, K. Liu, X. Du, H. Zang, Water-Weakening Effects on the Mechanical Behavior of Different Rock Types: Phenomena and Mechanisms, Applied Sciences 9 (2019) 4450. https://doi.org/10.3390/app9204450.
[18] Y. Mahmutoğlu, The effects of strain rate and saturation on a micro-cracked marble, Engineering Geology 82 (2006) 137–144. https://doi.org/10.1016/j.enggeo.2005.09.001.
[19] B. Vasarhelyi, K. Ledniczky, Influence of water-saturation and weathering on mechanical properties of Sivac marble, in: Paris, France, 1999: pp. 691–694.
[20] J. Zhu, J. Deng, F. Chen, Y. Huang, Z. Yu, Water Saturation Effects on Mechanical and Fracture Behavior of Marble, Int. J. Geomech. 20 (2020) 04020191. https://doi.org/10.1061/(ASCE)GM.1943-5622.0001825.
[21] T. Waragai, Influence of thermal cycling in the mild temperature range on the physical properties of cultural stones, Journal of Cultural Heritage 59 (2023) 171–180. https://doi.org/10.1016/j.culher.2022.12.001.
[22] S. Siegesmund, J. Menningen, V. Shushakova, Marble decay: towards a measure of marble degradation based on ultrasonic wave velocities and thermal expansion data, Environ Earth Sci 80 (2021) 395. https://doi.org/10.1007/s12665-021-09654-y.
[23] L.A. Ostrovsky, P.A. Johnson, Dynamic nonlinear elasticity in geomaterials, Riv. Nuovo Cim. 24 (2001) 1–46. https://doi.org/10.1007/BF03548898.
[24] J.A. Ten Cate, T.J. Shankland, Slow dynamics in the nonlinear elastic response of Berea sandstone, Geophys. Res. Lett. 23 (1996) 3019–3022. https://doi.org/10.1029/96GL02884.
[25] R.A. Guyer, P.A. Johnson, Nonlinear Mesoscopic Elasticity: Evidence for a New Class of Materials, Physics Today 52 (1999) 30–36. https://doi.org/10.1063/1.882648.
[26] P.A. Johnson, B. Zinszner, P. Rasolofosaon, F. Cohen-Tenoudji, K. Van Den Abeele, Dynamic measurements of the nonlinear elastic parameter α in rock under varying conditions: NONLINEAR ELASTIC PARAMETER IN ROCK, J. Geophys. Res. 109 (2004). https://doi.org/10.1029/2002JB002038.
[27] P. Johnson, A. Sutin, Slow dynamics and anomalous nonlinear fast dynamics in diverse solids, The Journal of the Acoustical Society of America 117 (2005) 124–130. https://doi.org/10.1121/1.1823351.

[28] K.E.-A. Van Den Abeele, Influence of water saturation on the nonlinear elastic mesoscopic response in Earth materials and the implications to the mechanism of nonlinearity, J. Geophys. Res. 107 (2002) 2121. https://doi.org/10.1029/2001JB000368.
[29] V.S. Averbakh, V.V. Bredikhin, A.V. Lebedev, S.A. Manakov, Nonlinear acoustic spectroscopy of carbonate rocks, Acoust. Phys. 63 (2017) 346–358. https://doi.org/10.1134/S1063771017030022.
[30] L. Gao, P. Shokouhi, J. Rivière, Effect of Grain Shape and Relative Humidity on the Nonlinear Elastic Properties of Granular Media, Geophysical Research Letters 50 (2023) e2023GL103245. https://doi.org/10.1029/2023GL103245.
[31] L. Gao, P. Shokouhi, J. Rivière, Effect of relative humidity on the nonlinear elastic response of granular media, Journal of Applied Physics 131 (2022) 055101. https://doi.org/10.1063/5.0073967.
[32] T. Weiss, P.N.J. Rasolofosaon, S. Siegesmund, Ultrasonic wave velocities as a diagnostic tool for the quality assessment of marble, Geological Society, London, Special Publications 205 (2002) 149–164. https://doi.org/10.1144/GSL.SP.2002.205.01.12.
[33] E. Sassoni, G. Graziani, G. Ridolfi, M.C. Bignozzi, E. Franzoni, Thermal behavior of Carrara marble after consolidation by ammonium phosphate, ammonium oxalate and ethyl silicate, Materials & Design 120 (2017) 345–353. https://doi.org/10.1016/j.matdes.2017.02.040.
[34] P.A. Johnson, Nonlinear Elastic Wave NDE I. Nonlinear Resonant Ultrasound Spectroscopy and Slow Dynamics Diagnostics, in: AIP Conference Proceedings, AIP, Golden, Colorado (USA), 2005: pp. 377–384. https://doi.org/10.1063/1.1916701.
[35] M.C. Remillieux, R.A. Guyer, C. Payan, T.J. Ulrich, Decoupling Nonclassical Nonlinear Behavior of Elastic Wave Types, Phys. Rev. Lett. 116 (2016) 115501. https://doi.org/10.1103/PhysRevLett.116.115501.
[36] C. Mechri, M. Scalerandi, M. Bentahar, Separation of Damping and Velocity Strain Dependencies using an Ultrasonic Monochromatic Excitation, Phys. Rev. Applied 11 (2019) 054050. https://doi.org/10.1103/PhysRevApplied.11.054050.
[37] L.A. Ostrovsky, P.A. Johnson, Nonlinear dynamics of rock: Hysteretic behavior, Radiophysics and Quantum Electronics 44 (2001) 450–464. https://doi.org/10.1023/A:1017953331645.
[38] C. Payan, T.J. Ulrich, P.Y. Le Bas, T. Saleh, M. Guimaraes, Quantitative linear and nonlinear resonance inspection techniques and analysis for material characterization: Application to concrete thermal damage, The Journal of the Acoustical Society of America 136 (2014) 537–546. https://doi.org/10.1121/1.4887451.
[39] P. Rasolofosaon, B. Zinszner, P.A. Johnson, Propagation des ondes élastiques dans les matériaux non linéaires Aperçu des résultats de laboratoire obtenus sur les roches et des applications possibles en géophysique, Rev. Inst. Fr. Pét. 52 (1997) 585–608. https://doi.org/10.2516/ogst:1997061.
[40] H. Yiming, D. Jianhui, Z. Jun, An Experimental Investigation of Moisture-Induced Softening Mechanism of Marble Based on Quantitative Analysis of Acoustic Emission Waveforms, Applied Sciences 9 (2019) 446. https://doi.org/10.3390/app9030446.
[41] K.S.W. Sing, R.T. Williams, Physisorption Hysteresis Loops and the Characterization of Nanoporous Materials, Adsorption Science & Technology 22 (2004) 773–782. https://doi.org/10.1260/0263617053499032.

Table 1 Impact of heating temperature on Carrara Gioia marble microstructure probed by mercury intrusion porosimetry.

Heating temperature	Total porosity (%)	Pore size distribution (% of total porosity)				
		0.01 – 0.1 μm	0.1 – 1 μm	1 – 10 μm	10 – 100 μm	> 100 μm
unheated	0.81	5.11	49.9	12.12	16.90	16.21
40 °C	1.07	3.78	55.38	14.81	14.14	11.77
65 °C	1.58	2.84	33.56	10.78	24.94	27.88
85 °C	1.61	2.46	40.96	24.37	20.82	11.40
105 °C	2.59	0.97	29.79	23.32	21.34	24.59

Supplementary material: NRUS data

Tables of the NRUS results for the different hygric states.

Table 2 Resonant frequency values during the first adsorption-desorption cycle

Resonant frequency f_0 (Hz) during adsorption (1st cycle)								
RH	12%	33%	44%	52%	66%	76%	86%	96%
unheated	6480.1 ± 0.7	6454 ± 4	6434.8 ± 0.4	6396 ± 7	6295 ± 3	6190 ± 7	6090 ± 20	5909 ± 8
40 °C	6337.5 ± 0.3	6315 ± 4	6303 ± 2	6283 ± 3	6225 ± 4	6156 ± 7	6080 ± 10	5910 ± 10
65 °C	5145 ± 6	5104 ± 5	5058 ± 3	4950 ± 20	4700 ± 10	4524 ± 7	4430 ± 10	4320 ± 10
85 °C	3890 ± 4	3862 ± 5	3824 ± 7	3758 ± 4	3620 ± 10	3510 ± 6	3450 ± 10	3400 ± 20
105 °C	3507 ± 6	3458 ± 5	3418 ± 9	3366 ± 5	3270 ± 10	3195 ± 4	3150 ± 10	3110 ± 10
Resonant frequency f_0 (Hz) during desorption (1st cycle)								
RH	12%	33%	44%	52%	66%	76%	86%	96%
unheated	6587 ± 2	6537 ± 7	6450 ± 10	6349 ± 5	6250 ± 10	6164 ± 5	6030 ± 20	5910 ± 30
85 °C	4128 ± 4	4045 ± 7	3907 ± 9	3757 ± 5	3648 ± 9	3580 ± 10	3480 ± 10	3423 ± 9

Table 3 Nonlinear parameter values during the first adsorption-desorption cycle

Nonlinear parameter α (x 10^3) during adsorption (1st cycle)								
RH	12%	33%	44%	52%	66%	76%	86%	96%
unheated	3.8 ± 0.5	5.1 ± 0.3	5.7 ± 0.3	7.0 ± 0.4	8.7 ± 0.6	11.0 ± 0.3	14 ± 1	16 ± 1
40 °C	4.8 ± 0.4	6.5 ± 0.2	7.1 ± 0.3	8.0 ± 0.4	9.4 ± 0.8	11.7 ± 0.3	14 ± 1	18.0 ± 0.9
65 °C	5.5 ± 0.6	7.7 ± 0.6	9.0 ± 0.4	11.5 ± 0.1	16 ± 1	18.2 ± 0.6	23 ± 3	25 ± 3
85 °C	9.5 ± 0.3	13.0 ± 0.4	15.5 ± 0.8	19.5 ± 0.5	26 ± 2	33 ± 2	39 ± 3	43 ± 2
105 °C	8 ± 1	10.9 ± 0.2	12.8 ± 0.6	16 ± 1	20 ± 2	24 ± 1	27 ± 3	32 ± 3
Nonlinear parameter α (x 10^3) during desorption (1st cycle)								
RH	12%	33%	44%	52%	66%	76%	86%	96%
unheated	4.13 ± 0.09	6.1 ± 0.2	8.0 ± 0.9	10.3 ± 0.5	13.7 ± 0.7	15.4 ± 0.4	18 ± 1	20 ± 0.6
85 °C	10 ± 1	16.5 ± 0.5	23 ± 1	33 ± 1	42 ± 3	45 ± 2	46 ± 2	48 ± 7

Table 4 Resonant frequency values during 10 adsorption-desorption cycles

Resonant frequency f_0 (Hz) during adsorption-desorption cycling											
Number of cycles		1	2	3	4	5	6	7	8	9	10
unheated	12% RH	6480.1 ± 0.7	6587 ± 2	6662 ± 7	6706 ± 7	6740 ± 7	6737 ± 8	6737 ± 7	6771 ± 9	6776 ± 8	6770 ± 10
	96% RH	5909 ± 8	6050 ± 40	6060 ± 10	6050 ± 20	6040 ± 20	6050 ± 20	6040 ± 40	6030 ± 50	6040 ± 20	6026 ± 5
40 °C	12% RH	6337.5 ± 0.3	/	6508 ± 7	6510 ± 8	6529 ± 8	6533 ± 8	6533 ± 10	6560 ± 10	6570 ± 10	6570 ± 20
	96% RH	5910 ± 10	/	6090 ± 20	6070 ± 20	6040 ± 20	6060 ± 20	6040 ± 30	6040 ± 40	6050 ± 20	6038 ± 4
65 °C	12% RH	5145 ± 6	/	5462 ± 6	5530 ± 10	5588 ± 8	5590 ± 10	5590 ± 20	5650 ± 10	5670 ± 10	5672 ± 9
	96% RH	4320 ± 10	/	4470 ± 10	4450 ± 10	4420 ± 20	4420 ± 10	4440 ± 20	4420 ± 40	4440 ± 20	4461 ± 2
85 °C	12% RH	3890 ± 4	4128 ± 4	4212 ± 5	4270 ± 10	4313 ± 2	4310 ± 10	4310 ± 20	4380 ± 20	4393 ± 9	4392 ± 7
	96% RH	3400 ± 20	3491 ± 9	3480 ± 10	3440 ± 8	3410 ± 20	3390 ± 10	3450 ± 50	3400 ± 100	3420 ± 20	3469 ± 4
105 °C	12% RH	3507 ± 6	/	3761 ± 1	3796 ± 9	3824 ± 3	3824 ± 9	3820 ± 20	3887 ± 8	3901 ± 4	3910 ± 3
	96% RH	3110 ± 10	/	3180 ± 20	3140 ± 30	3110 ± 30	3070 ± 10	3130 ± 40	3000 ± 100	3110 ± 30	3159 ± 5

Table 5 Nonlinear parameter values during 10 adsorption-desorption cycles

Nonlinear parameter α (x 10^3) during adsorption-desorption cycling											
Number of cycles		1	2	3	4	5	6	7	8	9	10
unheated	12% RH	3.8 ± 0.5	4.13 ± 0.09	4.1 ± 0.7	4.0 ± 0.7	3.8 ± 0.7	4.0 ± 0.6	4.0 ± 0.6	3.8 ± 0.4	3.9 ± 0.6	4.3 ± 0.03
	96% RH	16 ± 1	19 ± 1	19 ± 1	20 ± 2	20 ± 1	20 ± 2	21 ± 2	19 ± 4	19.0 ± 0.9	21 ± 2
40 °C	12% RH	4.8 ± 0.4	/	5.3 ± 0.9	5.7 ± 0.9	5.8 ± 0.9	6.1 ± 0.7	6 ± 1	6.1 ± 0.7	6.1 ± 0.9	6.2 ± 0.6
	96% RH	18.0 ± 0.9	/	17 ± 2	18 ± 1	19 ± 2	20.4 ± 0.6	21 ± 2	20 ± 3	19.8 ± 0.6	20 ± 2
65 °C	12% RH	5.5 ± 0.6	/	6 ± 1	6 ± 1	5 ± 1	6 ± 1	6 ± 1	5 ± 1	5 ± 1	6 ± 1
	96% RH	25 ± 3	/	25 ± 2	28 ± 1	28 ± 1	29 ± 1	31 ± 2	27 ± 4	29 ± 1	29.4 ± 0.9
85 °C	12% RH	9.5 ± 0.3	10 ± 1	10 ± 3	9 ± 3	9 ± 2	10 ± 3	9 ± 3	8 ± 2	9 ± 3	9 ± 3
	96% RH	43 ± 2	49 ± 4	47 ± 3	50 ± 5	48 ± 1	52 ± 3	53 ± 7	39 ± 6	49 ± 4	49 ± 5
105 °C	12% RH	8 ± 1	/	9 ± 2	9 ± 2	8 ± 2	10 ± 2	9 ± 2	9 ± 2	9 ± 2	9 ± 2
	96% RH	32 ± 3	/	31 ± 7	38 ± 2	38 ± 5	41 ± 2	42 ± 5	33 ± 4	40 ± 4	41 ± 3